

ABSTRACT

Title of Thesis: COLORIMETRIC NANOPARTICLES FOR BIOSENSING

Kankindi Rwego, Master of Science, 2014

Thesis directed by: Professor Peter Kofinas
Department of Bioengineering

In order to develop biosensors that change color upon the detection of a pathogen, nearly monodisperse polymer nanoparticles that can arrange into an ordered lattice structure that emits structural color, which is color free of pigment, or dye are synthesized. This work investigates methods for preparing electrostatically stabilized lattice structures by investigating the co-polymerization of polystyrene latex particles with the ionic co-monomer sodium-2-acrylamido-2-methylpropane sulfonate ("AMPS") through varying emulsion polymerization reaction parameters.

Additionally, this work is the first to deposit polystyrene-co-poly(N, N-dimethylacrylamide) core-shell nanoparticles onto a glass substrate, entrap in an elastomer matrix, and successfully show color change from green to red in less than 30 seconds upon exposure to a non-polar solvent. As such, the ability to induce a color change that is observable by the unaided human eye has been established. Therefore, this thesis promises to lead to the development of colorimetric biosensors in the near future.

COLORIMETRIC NANOPARTICLES FOR BIOSENSING

by

Kankindi Rwego

Thesis submitted to the Faculty of the Graduate School of the
University of Maryland, College Park in partial fulfillment
of the requirements for the degree of
Master of Science
2014

Advisory Committee:

Professor Peter Kofinas, Chair
Professor William Bentley
Associate Professor Isabel Lloyd

@Copyright by

Kankindi Rwego

2014

ACKNOWLEDGMENTS

I gratefully acknowledge Dr. Peter Kofinas for the opportunity to conduct this research project. I also acknowledge Omar Ayyub for his valuable conversations and suggestions regarding this work. I also acknowledge the support of the Maryland NanoCenter and its NispLab.

TABLE OF CONTENTS

1.0	Introduction	1
1.1	Motivation	1
1.2	Colorimetric Nanoparticles	4
1.3	Physical Laws	5
1.4	Dimensionality	9
1.5	Soft Sphere Model	11
1.51	Crystalline Colloidal Arrays	11
1.6	Hard Sphere Model	13
1.61	Synthetic Opals	13
1.62	Assembly of Synthetic Opals	14
1.63	Entrapment of Synthetic Opals in Gel Matrix	16
2.0	Synthesis of Monodisperse Polymer Spheres	17
2.1	Emulsion Polymerization	17
2.2	Crystalline Colloidal Arrays	19
2.3	Synthetic Opals	21
2.4	Assembly	22
2.5	Elastomer Entrapped Colorimetric Nanoparticles	23
3.0	Experimental Results and Discussion	23
3.1	Crystalline Colloidal Arrays	23
3.2	Synthetic Opals	27
4.0	Conclusions and Future Considerations	32
	Bibliography	34

1.0 Introduction

1.1 Motivation

This thesis introduces the phenomenon of structural color reflected by lattices of monodisperse spheres and explains the physical laws that control the emission of color without pigment or dyes. Additionally, this thesis investigates the synthesis and assembly of the Soft Sphere model and Hard Sphere model of monodisperse spheres, including a new deposition method for core-shell polystyrene-co-poly(N, N-dimethylacrylamide) nanoparticles onto a glass substrate. This thesis also reports on the entrapment of Hard Sphere model monodisperse spheres in a gel matrix designed to quickly change the color reflected from the spheres in response to the expansion or contraction of the gel matrix. Lastly, this thesis briefly previews future work on methods of functionalizing the biosensor to rapidly detect an analyte of interest. By laying this foundation, this work creates a platform for developing future biosensors which could be equipped to provide first responders, even personnel with limited training in limited resource settings, with a rapid and reliable method for monitoring disease outbreaks. The principles we establish from this work could ultimately lead to the development of responsive model biosensors that could form the basis for multiple or multiplexed “litmus test” diagnostic assays, configured as small “stickers,” large coating sheets, or even integrated into fabrics or coatings.

The envisioned biosensor platforms will have the potential to overcome many of the problems associated with the fabrication of diagnostic assays. Response time will be nearly instantaneous, overcoming the lag time inherent in traditional biosensors. The stability of such abiotic sensor platform will be greatly increased over their competing biological counterparts. These abiotic materials will not be subject to environmental (thermal, chemical, etc.) degradation that could alter the sensing capability of the final device. Importantly, these sensors would work unpowered, at ambient temperatures and pressures and physiological conditions without the need for electronics interfacing. As such, they would serve as stand alone sentinels. By eliminating the need for additional energy, such a system could provide a low-cost, lightweight, integrated sensor technology requiring no manipulation by the first responder, and having no logistics tail.

The first principle of Bragg diffraction-type structural color is found in nature. Some species maintain a decorative structural color as a way of attracting others, camouflaging themselves, warning to other predators, or a way of entrapping its prey. The iridescence found on peacock feathers and some beetles as well as the blue wing color of the Morpho butterfly are examples of natural nanostructures with periodicities on the order of the wavelength of light. In addition to simply having decorative structural color, some species are able to tune the color of their shells or scales in response to certain environmental conditions. For example, the damselfish is able to change its color from a bright blue to green depending on its environment.(1) Figure 1 is a schematic of how the damselfish uses a specialized cell called an iridophore that contains stacks of guanine crystal

nanoplates. Because the nanoplates' index of refraction is different from the surrounding cytoplasm of the iridophore cell, when the spacing between nanoplates is changed, the color changes from blue to green.

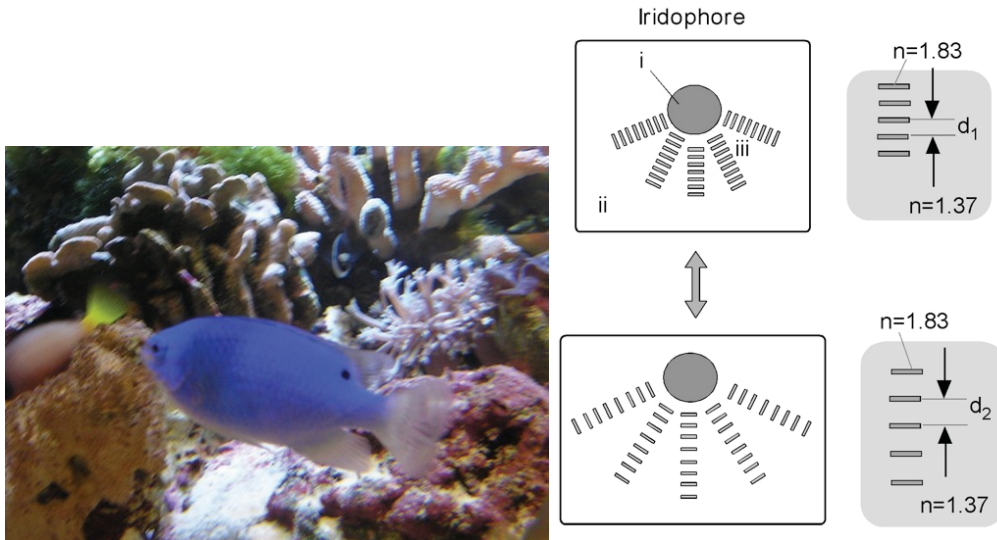


Fig. 1, Fudouzi H. Tunable structural color in organisms and photonic materials for design of Bioinspired materials. *Science and Technology of Advanced Materials*. 200; 12(6):064704

To produce colorimetric nanoparticles in the laboratory, emulsion polymerization is used to synthesize nearly monodisperse polymer particles that can arrange in an ordered structure producing a viewing angle-dependent color effect due to Bragg diffraction. The colorimetric nanoparticles are subsequently entrapped within a polymerized gel matrix such as an elastomer composite or a hydrogel. Elastomer composites swell or shrink reversibly when exposed to a hydrophobic solvent. Hydrogels are made from insoluble, cross-linked polymer network structures composed of hydrophilic homo- or hetero-co-polymers, which have the ability to absorb significant amounts of water.(2)

When an unconstrained macroscopic network polymer is swollen in a solvent, it undergoes swelling. On swelling, each network strand is stretched as the cross-linked

junctions move further apart. A fundamental concept for the intended biosensor is the diffraction of light at visible wavelengths as determined by lattice spacing, giving rise to an intense color. Upon subsequent recognition of an analyte and after changing or eliminating the crosslinks constraining the gel matrix, the gel will swell, increasing the mean distance of the lattice spacing, leading to a change of color. When the mean distance of the lattice spacing increases, the color is said to “red-shift” towards a larger-sized wavelength of light, where red is the color reflected at approximately 700 nm. When the mean distance decreases, the color is said to “blue-shift” towards a shorter wavelength of light, where blue is the color reflected at approximately 450 nm.

As such, the path to the ultimate goal of the above-described abiotic sensors requires a foundational understanding of the chemistry of colorimetric nanoparticles capable of forming structural color, the physics of the reflection of color without pigment or dyes, the variety of one-dimensional, two-dimensional, and three-dimensional arrangements of the lattices, with particular emphasis on the synthesis and assembly of three-dimensional Soft Sphere and Hard Sphere models of monodisperse spheres, and the entrapment of a lattice of monodisperse spheres inside a gel matrix.

1.2 Colorimetric Nanoparticles

A clear understanding of the type of colorimetric nanoparticles capable of assembling into a lattice structure is essential. The colorimetric nanoparticles investigated here consist of monodisperse spheres. According to the National Institute of Standards and Technology (“NIST”), monodisperse:

describes a dispersed system in which all the particles are of the same or nearly the same size, forming a narrow (unimodal) distribution about a median value; a particle distribution may be considered monodisperse if at least 90 % of the distribution lies within 5 % of the median size(3)

The nanoparticles are made of dielectric materials such as a polymer latex or silica particles. This thesis focuses on polystyrene as the main polymer used in the synthesis methods. Polystyrene has a higher refractive index ($n_{ri}=1.59$) than silica ($n_{ri}=1.54$).⁽⁴⁾ As the polymerization method investigated is an emulsion in water, polystyrene is followed by hydrophilic co-monomers such as sodium-2-acrylamido-2-methylpropane sulfonate (“AMPS”) and poly (N, N-dimethylacrylamide) (“acrylamide”). Additionally, the polystyrene emulsion polymerization procedures investigated are often one-pot methods.

A crystalline array of monodisperse spheres is a lattice structure composed of the nanoparticles in some media that has a refractive index that differs from the media. Once the lattice structure is formed, the nanoparticles emit structural color which is color free of pigment or dye which is **nearly** described by Bragg’s Law of Diffraction ($m\lambda = 2d\sin \theta$) with the following equation: $m\lambda = 2dn_{riavg}\sin \theta$, where m is the diffraction order, λ is the wavelength of light in a vacuum (also called a “stop band”), d is the diffracting plane spacing, n_{riavg} is the average refractive index of the system, and θ is the Bragg glancing angle.⁽⁵⁾

1.3 Physical Laws

The physics behind the structural color can be explained using an approximation called geometrical optics. In geometrical optics, light, in the form of

a ray, travels out from its source along straight lines.(6) Constructive interference occurs when rays of light are partially reflected from and partially transmitted through a crystalline array of spheres. Interference is the superposition of two or more individual wavelengths of light. Constructive interference is the additive superposition of individual wavelengths leading to an enhanced condition.

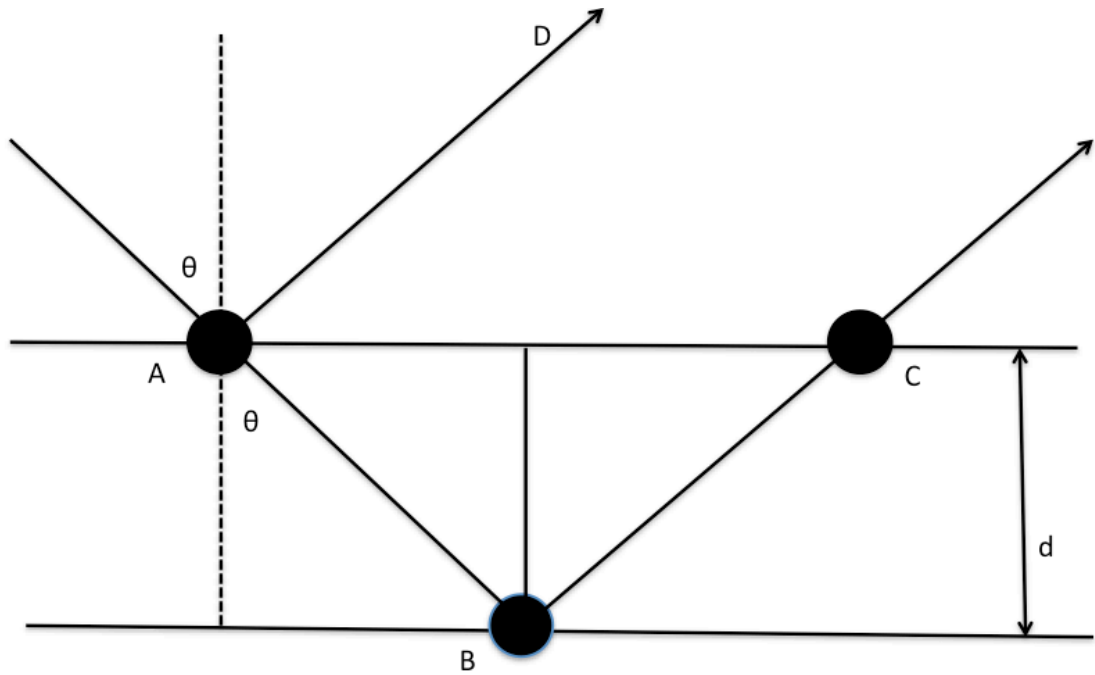


Fig. 2, Bragg's Law of Diffraction

Figure 2 is a schematic of Bragg's Law constructive interference of a lattice of monodisperse spheres. The colorimetric nanoparticles arrange themselves into lattice planes separated by a distance (d). Points A and C are on one plane and point B is on the plane below. The path difference between the ray that gets reflected along AD, (R_1) and the ray that gets transmitted and then reflected along AB and BC, (R_2) is:

$$R_2 - R_1 = (AB) + (BC) - (AD) \tag{1}$$

If this path difference is equal to an integer value, (m) of the wavelength, then R_1 and R_2 will constructively interfere:

$$m\lambda = (AB) + (BC) - (AD) \quad (2)$$

Bragg's Law of Diffraction is derived below:

$$AB = BC = \frac{d}{(\sin \theta)} \quad (3)$$

$$AC = \frac{2d}{(\tan \theta)} \quad (4)$$

$$\begin{aligned} AD &= AC \times (\cos \theta) = \frac{2d}{(\tan \theta)} \times (\cos \theta) = (2d) \times \left(\frac{\cos \theta}{(\sin \theta)}\right) \times (\cos \theta) \\ &= (2d) \times \frac{(\cos^2 \theta)}{\sin \theta} \end{aligned} \quad (5)$$

Returning to Equation 2:

$$m\lambda = \frac{d}{(\sin \theta)} + \frac{d}{(\sin \theta)} - (2d) \times \frac{(\cos^2 \theta)}{\sin \theta} \quad (6)$$

Equation 6 simplifies to:

$$m\lambda = \frac{2d}{(\sin \theta)} - (2d) \times \frac{(\cos^2 \theta)}{(\sin \theta)} \quad (7)$$

$$m\lambda = \frac{(2d) \times (1 - \cos^2 \theta)}{(\sin \theta)} = \frac{(2d) \times (\sin^2 \theta)}{(\sin \theta)} = 2d \sin \theta \quad (8)$$

The Bragg Diffraction Equation simplifies to the following:

$$m\lambda = 2d \sin \theta \quad (9)$$

The Bragg Diffraction Equation is modified, however, to take into account the reduced angle at which a ray is transmitted through a higher refractive index

material. The medium's average refractive index (n_{riavg}) of the lattice structure made of polystyrene spheres in water is:

$$n_{riavg} = n_2 f_2 + n_1 f_1 \quad (10)$$

Where n_1 represents the refractive index of water, n_2 represents the refractive index of the higher index media polystyrene and f_2 and f_1 represent the volume fractions occupied by the spheres and the water respectively. Generally, a more dense dielectric material has a larger refractive index, and as such, a first-order rule of mixtures is appropriate for determining the average refractive index (n_{riavg}). (7)

To derive the modified Bragg equation, one must combine Bragg's Law with Snell's Law of Refraction. Snell's Law states that a ray of light is transmitted through the lattice structure at an angle of refraction (ϕ) that is directly proportional to the sine of the angle of incidence (θ):

$$\frac{\sin \theta}{\sin \phi} = \frac{n_2}{n_1} \quad (11)$$

Because n_2 is larger than n_1 , the angle of refraction (ϕ) is reduced, which after some calculation, gives a slightly modified Bragg Diffraction equation:

$$m\lambda = 2dn_{riavg} \cos \phi \quad (12)$$

$$\sin \phi = \frac{1}{n_{riavg}} \sin \theta \quad (13)$$

$$1 - \sin^2 \phi = 1 - \frac{\sin^2 \theta}{(n_{riavg})^2} = \cos^2 \phi \quad (14)$$

$$m\lambda = 2d\sqrt{(n_{riavg})^2 - \sin^2 \theta} \quad (15)$$

Which is also often expressed as:

$$m\lambda = 2dn_{riavg} \sin \theta \quad (16)$$

Tunable Color

The modified Diffraction equation illustrates that the wavelength of light diffracted from a crystalline array of colorimetric nanoparticles is directly proportional to the lattice constant, (d) which refers to the spacing between the monodisperse spheres. The average refractive index contrast (n_{riavg}) between the surrounding material and the lattice also affects the color emitted from the surface of the monodisperse spheres. Additionally, the “filling factor” or the volume of the nanoparticle spheres (f_2) compared to the volume of the surrounding material water (f_1) will also impact color.(8)

1.4 Dimensionality

One-dimensional (“1D”), two-dimensional (“2D”), and three-dimensional (“3D”) monodisperse spheres can be found in nature as well as made in the laboratory. In Figure 3, below, the diagram shows (A) the 1D periodicity in the green and purple neck feathers of domestic pigeons; (B) the 1D periodicity found in the wings of Morpho butterflies; (C) the 2D photonic crystal structure in the barbules of male peacocks’ feathers; (D) the 2D periodicity of the cylindrical voids found in the iridescent setae from polychaete worms; (E) the 3D inverse opal structures in *Parides sesortris*; and (F) the 3D diamond-like crystal structure found in the shell of the beetle *L. augustus*.(9)

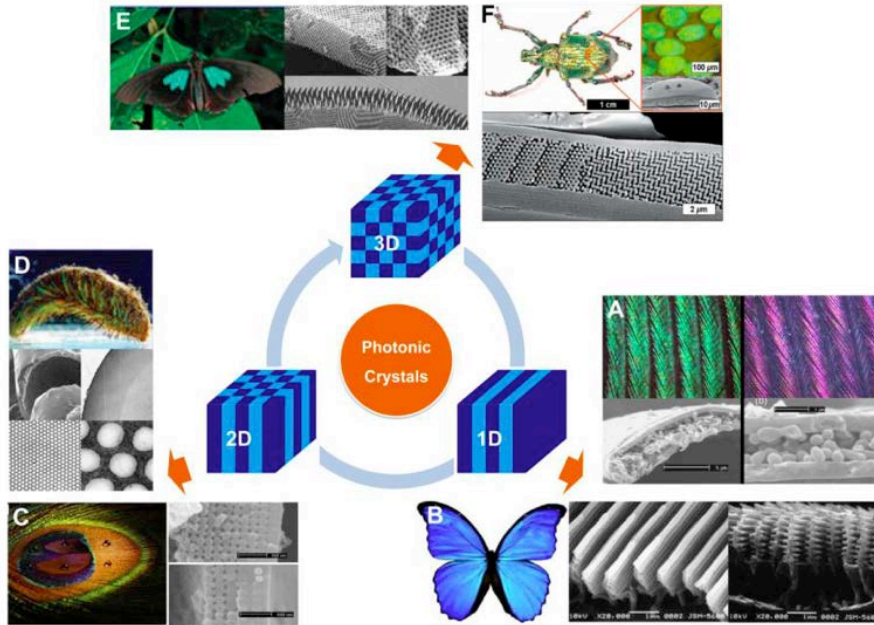


Fig. 3, Wang H, Zhang KQ. Photonic crystal structures with tunable structure as colorimetric sensors. *Sensors*. 2013; 13(4); 4192-213

In the laboratory, making 1D systems involves deposition of layers of dielectric materials. The optical contrast comes from the differing dielectric indices of the materials. 2D systems are similarly made, however, the second dimension arises from the selective removal of the top layer dielectric material to reveal the substrate below. This thesis involves some of the methods for making 3D monodisperse spheres.

Three-dimensional monodisperse spheres can form crystalline lattice structures based on two different principles of formation: the Soft sphere model and the Hard sphere model.(10)

1.5 Soft Sphere Model

1.5.1 Crystalline Colloidal Arrays

The Soft-sphere model applies to the formation of a crystalline colloidal array (“CCA”) composed of nanoparticles each having surface charges such that the individual particles repel each other. Colloidal crystals are made of monodisperse, concentrated, highly charged spheres in a very low ionic strength liquid media are macroscopically ordered non-close-packed arrays, forming a colloidal fluid.(11) The surface charges in the Soft-sphere model cause long-range repulsions. As such, the CCA is self-assembled by maximizing the distance between nanoparticles and by also minimizing the repulsion between them. Consequently, the CCAs have a greater range of volume fractions.

The lattice structure is formed of relatively largely spaced colloidal spheres suspended in water. The distance between the spheres is much larger than the individual particle diameter. The interparticle distance is set by the electrostatic repulsion caused by the charged particles. When the spacing ($d_1 \rightarrow d_2$) between the charged particles is changed, the stop band or color reflected off the surface of the colloidal crystal changes.

Creating a crystalline colloidal array based on repulsive electrostatic interactions is complex. Experimental conditions such as temperature, particle size monodispersity, surface charge density, particle number density, and the presence of counter ions in the colloidal suspension all impact a CCA’s ability to self-assemble and subsequently Bragg diffract light.(12)

This work modifies the preparation of monodisperse highly charged polystyrene spheres suspended in water previously documented by S.A. Asher at the University of Pittsburgh.(13) According to Asher's protocol, the emulsion polymerization calls for the use of styrene, divinyl benzene ("DVB"), sodium 1-allyloxy-2-hydroxypropane sulfonate ("COPS-1"), sodium di-1, 3- dimethylbutyl sulfosuccinate in isopropanol and water, sodium bicarbonate, and ammonium per sulfate ("APS").

Styrene is the main monomer that makes up the polymer nanoparticles. DVB is used in small amounts in order to cross-link the monomer units. Because sodium 1-allyloxy-2-hydroxypropanesulfonate ("COPS-1") is a proprietary ionic co-monomer, sodium-2-acrylamido-2-methylpropane sulfonate ("AMPS"), a more readily available ionic co-monomer, is investigated instead. It is hypothesized that AMPS co-polymerizes with styrene to form an ionic polymer having a negative surface charge. In fact, the extent, if any, of co-polymerization is investigated. Additionally, even though Asher called for sodium di-1, 3- dimethylbutyl sulfosuccinate in isopropanol and water, the available sodium dihexyl sulfosuccinate ("MA-80") as the surfactant is utilized instead.

Moreover, Asher's protocol is altered in response to the availability of certain equipment. Thus, as a jacketed cylindrical reaction vessel is unavailable, some changes to the recipe, including injecting, prior to commencing polymerization, the water-soluble initiator in only 1 ml of purified water as opposed to 10 ml are utilized in order to better control temperature fluctuations. Additionally, dialysis of

the emulsion polymerization product for not more than seven days instead of the 14-21 days called for in the protocol is conducted.

1.6 Hard Sphere Model

1.6.1 Synthetic Opals

The Hard-sphere model describes solid cubic close-packed arrays such as opals. A natural opal is a close-packed array of monodisperse colloidal silica spheres. Opals Bragg diffract light, emitting an iridescent color called opalescence.(14)

The synthesis of opals can involve the use of two or more polymers. One recent method published by Ma et al. in 2013 utilizes the co-polymerization of styrene and acrylamide.(15) Because styrene is hydrophobic and because acrylamide is hydrophilic, the final product has the form of a hard styrene core with acrylamide brush structures. These brush structures are often referred to as a “shell.” The formation of the core-shell nanoparticles helps set the particle distance between the close-packed particles. When the amide side groups located in the shell interact with water, the acrylamide shell expands, thereby changing the lattice spacing and “red-shifting” color. This color change, however, was **only observable** after centrifuged-induced assembly of the colloidal spheres into a solid pellet. (15) This work is the first to deposit polystyrene-co-poly(N, N-dimethylacrylamide) core-

shell nanoparticles onto a glass substrate, entrap in an elastomer matrix, and successfully show color change upon exposure to a non-polar solvent.

1.62 Assembly of Synthetic Opals

The assembly of synthetic opals is entropy-driven and relatively simple. The lattice structure forms by minimizing dead space. As such, the crystalline structure occurs over a very narrow range of volume fractions, (f) the maximum theoretical volume fraction occurs at $f=0.74$. Assembly methods under the Hard-sphere model include centrifugation, filtration, electrophoresis deposition, horizontal deposition, vertical deposition, spin-casting, and surface pattern-assisted deposition, among others.(16)

Although centrifugation is a simple way to force the assembly of synthetic opals, centrifugation is not useful for reaching the goal of developing portable, low-cost and easy-to-use model biosensor. Consequently, this thesis investigated the novel crystallization of core-shell polystyrene-co-poly(N, N-dimethylacrylamide) nanoparticles onto a solid substrate using convection wherein capillary action and evaporation drive self-assembly. According to Fudouzi et al., a uniform and flat film of colloidal spheres will crystallize on a hydrophilic glass slide if the suspension of colloidal spheres is also completely covered with a hydrophobic silicone layer.(17)

This method involves placing a cleaned glass substrate onto a clock dish (also called a watch glass). After carefully dropping the colloidal suspension onto the cleaned and hydrophilic glass substrate, the entire suspension is covered with a silicone liquid. The theory behind the crystallization is that capillary action assisted

by water evaporation forces the assembly into closely packed colloidal particles. A suspension of a close-packed array of nanoparticles is fluid at low particle volume fractions but crystallizes to a close-packed crystal structure for a volume fraction, $f > 0.545$. Here, it is demonstrated that the deposition of core-shell nanoparticles is as feasible as the deposition of hydrophobic polystyrene spheres as originally called for in the Fudouzi method. Additionally, this work changes the method by utilizing the similarly viscous curing agent (Part B) of a poly (dimethylsiloxane) PDMS elastomer kit from Dow Corning (Sylgard 184) instead of silicone (GE silicone SF96; viscosity, 50 cSt). This change is significant because it shows that the curing agent (part B) has a similar specific gravity as the silicone (0.97 g/ml), which is lighter than that of water (1.00 g/ml) and lighter than that of polystyrene-co-poly (N, N-dimethylacrylamide).

Future considerations include investigating different deposition methods in order to have the ability to develop multiple or multiplexed “litmus test” diagnostic assays. Because the synthetic crystals have a hydrophobic polystyrene core and a hydrophilic acrylamide shell, the colloidal spheres can be deposited onto a hydrophobic surface using surface pattern-assisted deposition. Moreover, one such type of surface pattern-assisted deposition includes ink jet printing. The acrylamide hydrophilic shell assists the lattice arrangement during ink-jet printing onto a hydrophobic substrate because the hydrophilic acrylamide soft-shells merge together and the lattice is deposited via a “surface-tension-confined channel.” (4) Subsequently when the ink is evaporated off, a bright green monochromatic color is displayed.

1.63 Entrapment of Synthetic Opals in Gel Matrix

An important principle of the intended biosensor is that a distinct and reversible color change is visible by the unaided eye. This thesis investigates entrapping the synthetic opal crystals into an elastomer composite in order to manipulate the lattice spacing (d). The curing agent used in the previous crystallization process (Section 1.62) is first removed. The same PDMS elastomer kit (Sylgard 184) is used again. The base material (Part A) is diluted with DMS-T00, a much less viscous silicone fluid before mixing with the curing agent (Part B). The mixed PDMS elastomer is poured over the green deposited synthetic opal and, over time, the voids of the synthetic opal lattice are filled with the PDMS through capillary action. Because PDMS swells in a non-polar solvent such as isopropyl alcohol, hexane, and chloroform, the lattice spacing (d) increases and the color of the synthetic crystal red-shifts. Upon evaporation of the solvent, the PDMS elastomer shrinks and the entrapped synthetic crystal blue-shifts.(18)

Future considerations also include investigating a variety of cross-linking monomers mixed into the elastomer composite in order to have the cross-links strategically cleaved, expanding the gel, and increasing the lattice structure of the entrapped giving way to an observable, distinct red-shifting. One such potential method involves the detection of oligonucleotides via a preferential affinity process.(19) By adding hybridized dioligonucleotides with a 10 base pair complementary regions flanked by additional base pairs into a gel matrix network, probe oligonucleotides can then displace the original complement. Competitive

hybridization of the oligonucleotides can change the length of the crosslinks, and thereby causing the gel matrix to swell and to red-shift.

2.0 Synthesis of Monodisperse Polymer Spheres

The preparation of both Soft Sphere (CCA) and Hard Sphere (synthetic opal) models both involve emulsion polymerization. While the synthetic opal method involves an additional assembling step, however, the synthesis of synthetic opals is less complex than forming crystalline colloidal arrays. As a result, the synthetic opal colorimetric nanoparticles are entrapped in a gel matrix in order to progress towards building the desired colorimetric biosensor.

2.1 Emulsion Polymerization

Emulsion polymerization is a free radical polymerization that takes place in an emulsion consisting of water, monomer, surfactant and other additives. A surfactant is comprised of a long, linear, non-polar (hydrophobic) “tail” with a polar (hydrophilic) “head” which lowers the surface tension of water and allows the hydrophobic components to form an emulsion in water. According to the Smith-Ewart-Harkins theory for the mechanism of free-radical emulsion polymerization, a monomer is dispersed or emulsified in a solution of surfactant and water forming relatively large droplets of monomer in water.(20) Prior to the polymerization reaction, the surfactant is mixed with water using a mechanical stirrer. The individual surfactant

molecules will surround the monomer units. The hydrophobic tails of the surfactant molecules will adsorb onto the monomer units and the hydrophilic surfactant head will face the water medium. Additionally and with the help of stirring, small amounts of monomer diffuse through the water to the micelle. A micelle is an aggregate of surfactant molecules wherein the polar (hydrophilic) "head" of each surfactant molecule faces the surrounding water and the non-polar hydrophobic "tail" of each surfactant molecule is sequestered in the micelle center.

A water-soluble initiator is then introduced into the water phase where it reacts with monomer in the micelles. The initiator decomposes to form free radicals. In order to optimize the available free radicals, oxygen must be prevented from entering the system by introducing nitrogen gas. As the total surface area of the micelles grows to be much greater than the total surface area of the fewer, larger monomer droplets; the initiator radicals typically react in the micelle and not the monomer droplet. Monomer in the micelle quickly polymerizes and the growing chain terminates. At this point the monomer-swollen micelle has turned into a polymer particle. Eventually, both monomer droplets and polymer particles are present in the system. As polymerization proceeds, more monomer from the droplets diffuses to the growing particle, where more initiators will eventually react. Eventually the free monomer droplets disappear and all remaining monomer is located in the particles.

2.2 Crystalline Colloidal Arrays

The materials used in this process are shown below in Table 1:

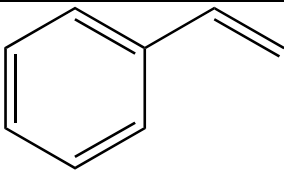
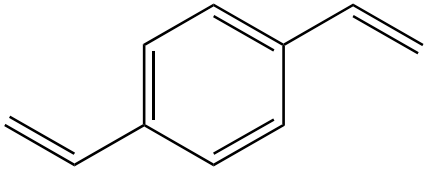
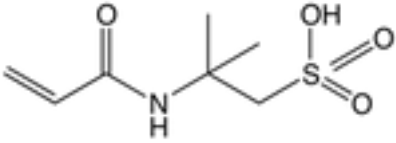
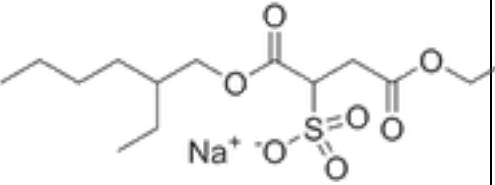
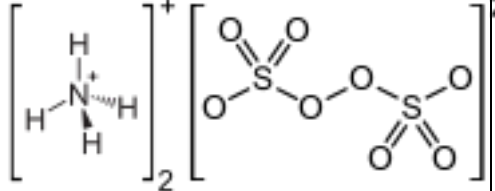
Material	Function	Structure
Styrene ($C_6H_5CH=CH_2$)	Monomer	
Divinyl Benzene ($C_{10}H_{10}$)	Cross-linker	
AMPS	Ionic co-monomer	
MA-80	Surfactant	
APS	Radical Initiator	

Table 1, Materials used in the synthesis of crystalline colloidal arrays

The experimental set up for this emulsion polymerization utilizes a four-neck 250 ml round bottomed flask reaction vessel, reflux condenser, mechanical stirrer with a Teflon blade, temperature sensor, and a nitrogen gas/ reagent inlet. The

reaction vessel is immersed in a silicon oil bath that sits upon a combination hot plate and magnetic stirrer.

Before beginning, the inhibitor in styrene and divinyl benzene (“DVB”) is removed by adding aluminum oxide under stirring and decanting off the monomer after one hour. Additionally, 45 ml purified deionized water and 86 mg sodium bicarbonate mixture is purged with nitrogen gas for thirty (30) minutes. The 37.5 ml and 1.5 ml of de-inhibited monomers styrene and DVB respectively are mixed together and then purged with nitrogen gas for twenty (20) minutes.

The water and sodium bicarbonate mixture are added to the reaction vessel. Then, 15 ml of MA-80 is added. The purged styrene and DVB mixture is housed in an addition funnel connected to four-neck round bottom flask. At this time the reaction vessel is heated to 50°C and stirred at a rate of 125 RPM. Once the temperature probe reads 50°C, the stir rate is increased to 350 RPM and styrene and DVB are introduced into the reaction vessel as a drizzle. After approximately five (5) minutes to drizzle in the monomers, 1.38 g of the ionic co-monomer dissolved in 5 ml of water is injected into the reaction vessel.

The reaction vessel is then heated to 70°C, and at a stable 70°C, 375 mg of initiator APS dissolved in 1 ml water is injected into the emulsion. The emulsion polymerization reaction is allowed to proceed for three hours. After cooling the resultant milky white liquid product, the product was filtered, dialyzed against water for one week, and then further purified with an ion-exchange resin.

2.3 Synthetic Opals

These synthetic opals are composed of polystyrene copolymerized with N, N-dimethylacrylamide to create a “core-shell” structure. Preparation of the synthetic opals utilizes N, N-dimethylacrylamide (“acrylamide”), sodium dodecyl sulfate (“SDS”), styrene, potassium persulfate (“KPS”), and purified deionized water.

Styrene’s inhibitor is removed by adding aluminum oxide under stirring and decanting off the monomer after one hour. While removing the inhibitor, the emulsion polymerization apparatus is set up; the experimental set up for this emulsion polymerization utilizes a four-neck 250 ml round bottomed flask reaction vessel, a reflux condenser, a mechanical stirrer with a Teflon blade, a temperature sensor, and a nitrogen gas/ reagent inlet. The reaction vessel is immersed in a silicon oil bath that sits upon a combination hot plate and magnetic stirrer.

130 ml of purified deionized water is then added to the reaction vessel. Next, a mixture of 30 ml purified deionized water, 5 ml of styrene, 2 ml of acrylamide, and 0.005 g of SDS is added to the reaction vessel. The water, styrene, acrylamide, and SDS are stirred at 300 RPM under nitrogen gas for thirty (30) minutes. After purging, the reaction vessel is heated to 70°C. At stable 70°C, a mixture of 0.15g KPS in 20 ml purified deionized water is injected into the reaction vessel. The emulsion polymerization reaction is allowed to proceed for 8 hours.

The milky white water-particle mixture is cleaned by repeating, four times, a water wash procedure which consists of: centrifuging the product, decanting the supernatant, replacing the supernatant with purified deionized water and re-

dispersing with a vortex. The centrifuged and decanted product forms a multicolored solid pellet.

2.4 Assembly

The re-suspended liquid product is dropped on cleaned aminated glass slides. The Gold Seal #3039 Ultrastick/ultrafast adhesion slides have amine groups attached and were purchased from Electron Microscopy Sciences. The glass slides are cut to approximately 25 mm by 25 mm and then are sequentially cleaned under sonication for ten minutes with soapy water, acetone, and 2-propanol. Afterwards, the slides are rinsed well with purified deionized water and then dried with a stream of nitrogen gas. The cleaned glass slides are each placed on a 65mm diameter Pyrex watch glass. 750 μ l of the colloidal sphere product is dropped on a glass slide. 2 ml of the curing agent (part B) of the poly (dimethylsiloxane) PDMS elastomer kit from Dow Corning (Sylgard 184) is dropped on top of the colloidal sphere product. Over the course of 24 hours, while sitting on the laboratory bench top at ambient room temperature, the water in the liquid product slowly evaporates and colorimetric nanoparticles assemble into a green close-packed solid crystal deposited on the glass substrate. The excess curing agent covering the crystal is wiped off with Kim-Wipes.

2.5 Elastomer Entrapped Colorimetric Nanoparticles

Using the PDMS elastomer kit from Dow Corning (Sylgard 184)), 2ml of the elastomer (part A) is placed in a small beaker to which 4 ml of DMS-T00 Silicone from Gelest is added. Next, 400 μ l of the curing agent (part B) is thoroughly mixed into the beaker. After mixing, the mixture is carefully poured onto the crystallized opal that is allowed to sit on the laboratory bench top for twenty-four hours. Afterwards, the PDMS is placed in a 55 ° C oven for 6 hours.

3.0 Experimental Results and Discussion

Experimentation with emulsion polymerization reactions is directed at synthesizing crystalline colloidal arrays (charged, macroscopically-ordered colorimetric nanoparticles) and closed-packed colorimetric nanoparticles (synthetic opals). Producing synthetic opaline crystals proved to be less complex than the development of CCAs.

3.1 Crystalline Colloidal Arrays

During emulsion polymerization, the temperature readings from the probe inserted in the reaction vessel would oscillate from 5 to 10 degrees Celsius above and below the targeted 70°C polymerization temperature. This was exacerbated by the final injection of water-soluble initiator dissolved in 10 ml of water. In Figure 4, below, a Transmission Electron Microscopy (“TEM”) image shows polystyrene particles averaging 92.28 nm in diameter. It is notable that the particles do not have a spherical morphology and are not monodisperse. Injecting APS dissolved in only 1

ml water, however, does diminish temperature fluctuations and allows polymerization to proceed at close to 70°C (+/- 5°C).

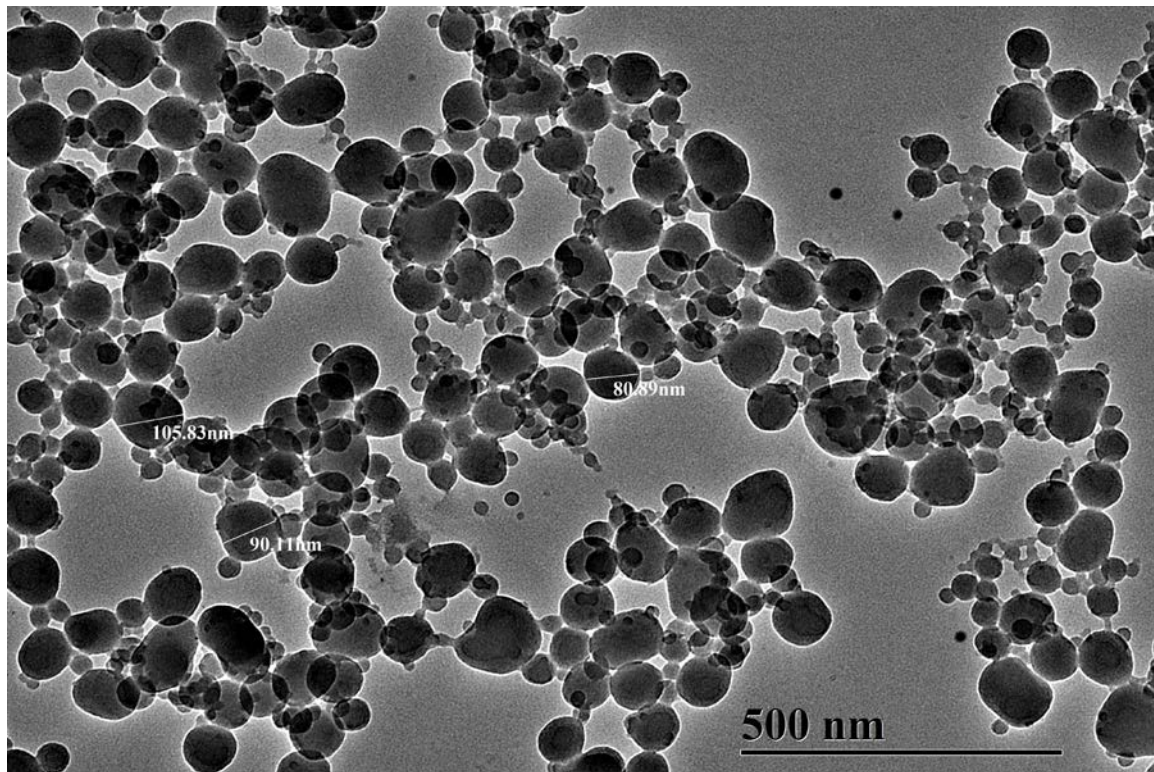


Fig. 4, TEM of emulsion polymerization of polystyrene with APS in 1 ml water

Another concern in the synthesis of CCAs is to produce spherical shaped 100 nm or greater-sized nanoparticles that are co-polymerized with an ionic co-monomer. Figure 5 shows a Scanning Transmission Electron Microscopy (“STEM”) image of an emulsion polymerization product after increasing the surfactant concentration from 8.25 ml (in Figure 4) to 15 ml surfactant. The particles are noticeably more spherical. However, no Bragg Diffraction is observable.

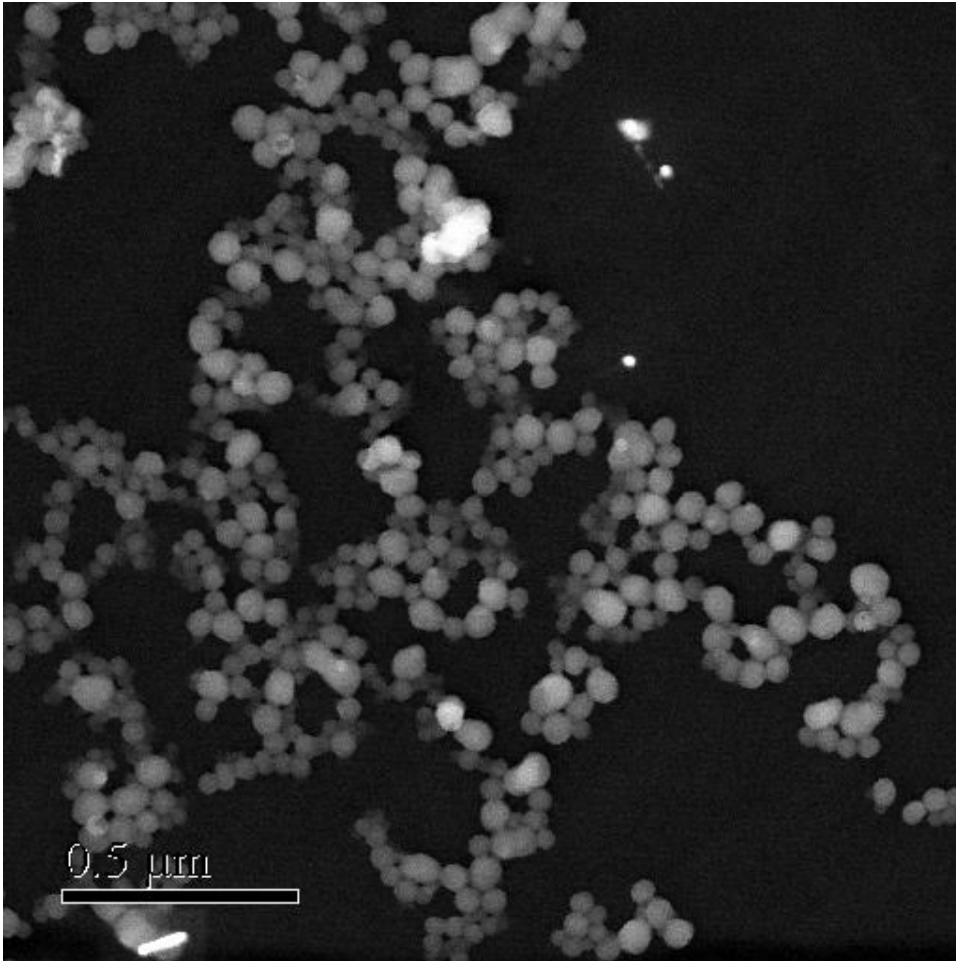


Fig. 5, STEM image of emulsion polymerization of polystyrene with 15 ml surfactant. This same emulsion polymerization product was characterized with Energy Dispersive Spectroscopy (“EDS”) to detect the level of sulfur as an indirect way to quantify the co-polymerization of AMPS based its on sulfonate groups. EDS showed that almost no sulfur present: 0.39 weight percent sulfur and 0.15 atomic percent sulfur.

It is likely, therefore, that AMPS may not be an adequate substitute for COPS-1 as a negatively charged co-monomer. Further supporting this conclusion are studies by Peiffer et al. on the reaction ratios in the copolymerization of polystyrene and AMPS.(21) According to Peiffer et al, utilizing a ratio of 95:5 styrene to AMPS in

DMF yields a product with 4.1 mole percent AMPS and 1.16 weight percent sulfur. Utilizing such a ratio means a four-fold increase of AMPS to the recipe. This change proves to interfere with the emulsion stability and rapidly forms a gel early on in the polymerization reaction. Figure 6 is a TEM image of the emulsion product made with 4.4g of AMPS. Figure 6 shows the poor morphology and evidence of coagulation and/or aggregation of particles. Interestingly, the EDS taken of that sample showed a significant increase in the amount of sulfur: 23.41 weight percent sulfur and 15.87 atomic percent sulfur.

Given that the sample has no observable indication of high sulfur content (no pungent smell, no yellow color), this high EDS reading indicates an artifact in the acquisition of the data, including a likely improper focusing of the electron beam on a sample area of unusually high sulfur content. Thus, although it is possible that the AMPS substitution is enough to interfere with the delicate balance of experimental conditions necessary for forming a CCA capable of reflecting color, further experimentation with the recipe and the utilization of other sulfur characterization tools may yield sufficient co-polymerization of the ionic co-monomer. Additionally, more experiments are needed in order to optimize morphology and size monodispersity as well. As such, more investigations into optimizing the size, morphology, and co-polymerization of polystyrene with AMPS in order to form electronegatively stabilized crystalline colloidal arrays is needed.

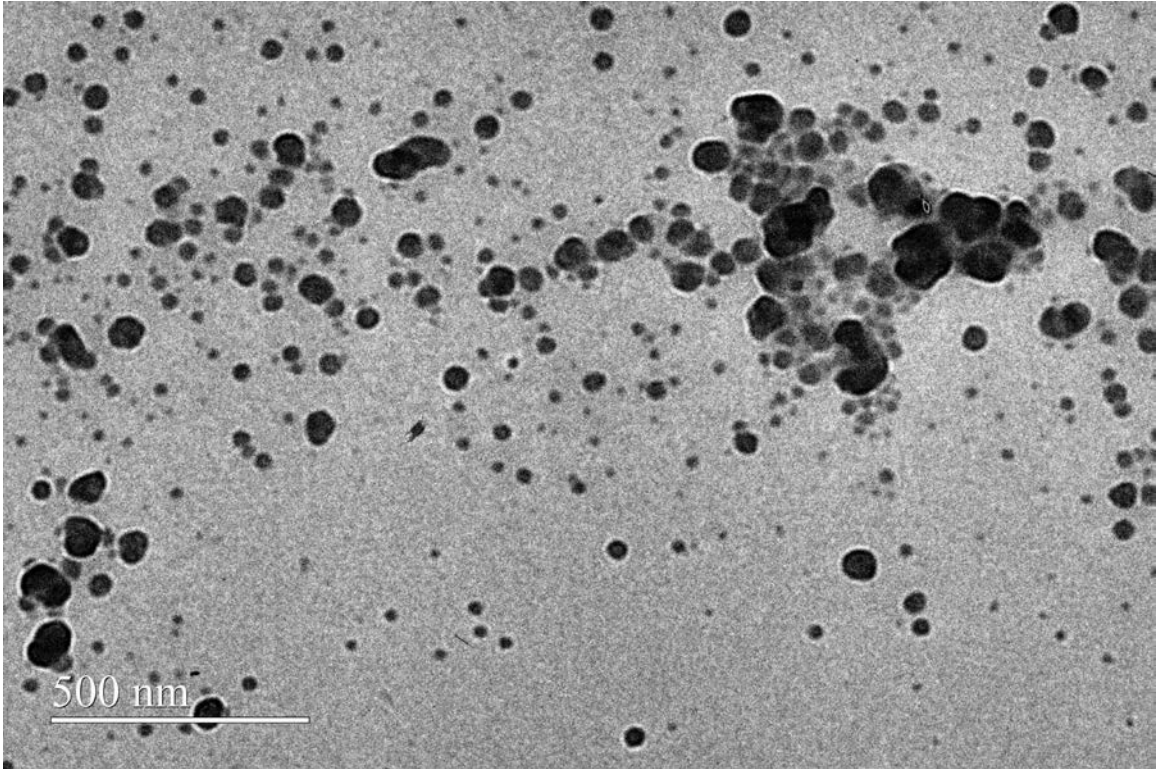


Fig. 6, TEM image of emulsion polymerization with 95:5 polystyrene: AMPS

3.2 Synthetic Opals

After the centrifuge wash and dialysis, the synthetic opals display an assortment of brilliant colors upon centrifugation down to a solid pellet. Figure 6 shows the pellet inside a curved centrifuge Eppendorf tube. Because the tube is curved and because there are multiple planes upon which the nanoparticles crystallize, multiple colors are observable.

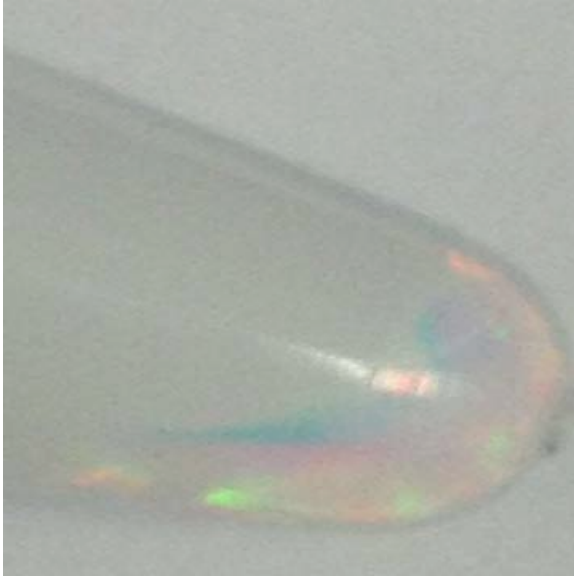


Fig. 7, Centrifuge tube containing opalescent polystyrene-co-poly (dimethylacrylamide) crystals

Using transmission electron microscopy to determine the shape and size of the nanoparticles. It is observed in figures 8 and 9 that the particles are approximately 208 nm in diameter each and they are sufficiently monodisperse to assemble onto a substrate and form a monochromatic color.

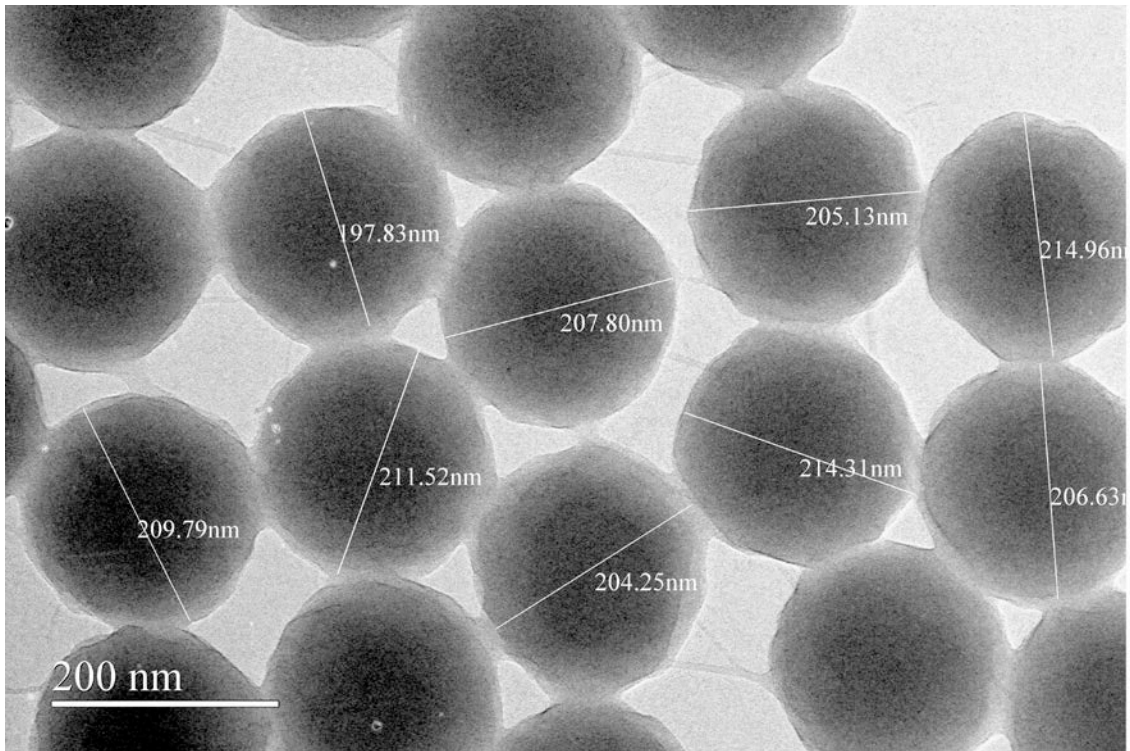


Fig. 8, Polystyrene-co-poly (dimethylacrylamide) core-shell nanoparticles

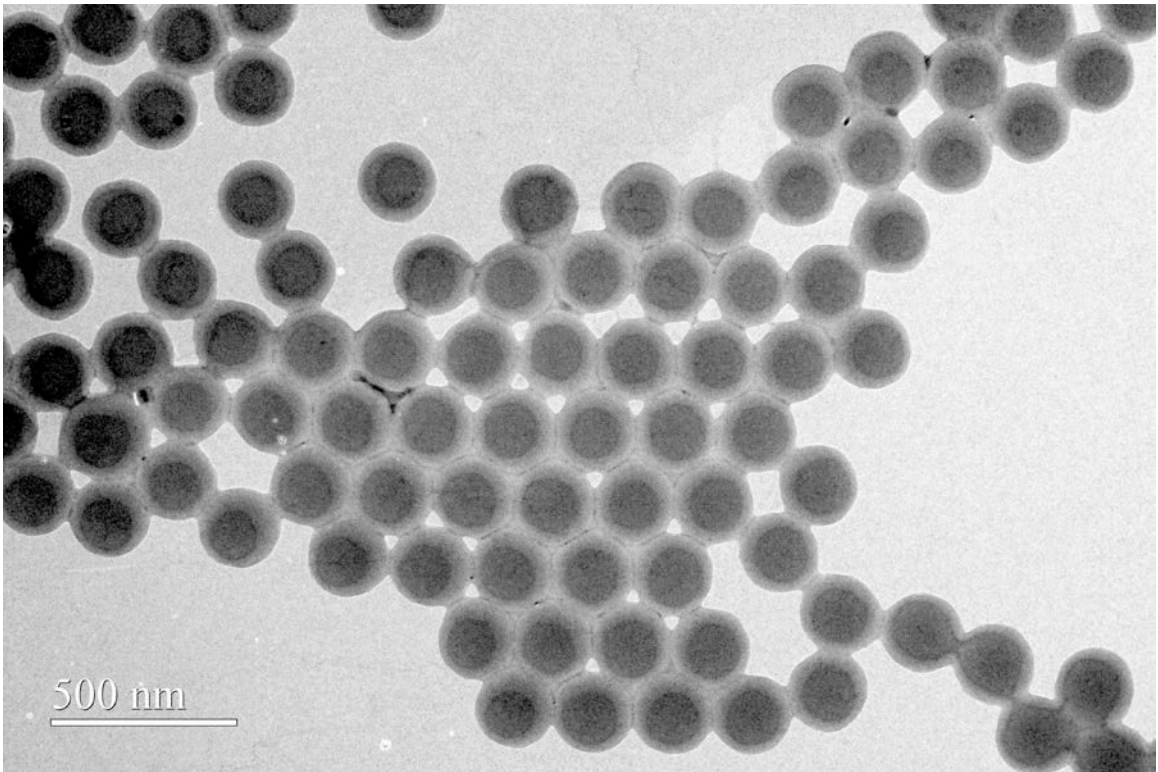


Fig. 9, Polystyrene-co-poly (dimethylacrylamide) core-shell nanoparticles

Below, in figure 10 is the bright green color displayed by the opalline crystals after crystallization and entrapment in PDMS. Figure 10 shows the approximately 25 mm by 25 mm glass slide placed on top of a watch glass and sitting on the black laboratory bench top. The photograph was taken with a camera phone from directly above the glass slide.

In approximately 30 seconds after dropping 100 μ l of chloroform onto the PDMS entrapped synthetic opal, the PDMS network swells and the synthetic opal changes color from bright green to red. After about three minutes, as seen in Figure 11 below, the PDMS network begins to shrink as the chloroform evaporates and the edges of the circle left by the drop are turning back to green. In the center of the circle, where it is likely chloroform was most dense, the PDMS film appears clear as

if it red-shifted so far as to move beyond visible light and/or destroy the lattice structure.



Fig. 10, PDMS entrapped polystyrene-co-poly (dimethylacrylamide) core-shell nanoparticles

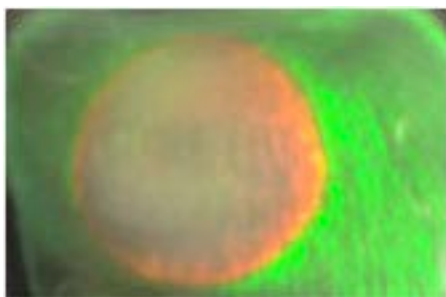


Fig. 11, Three minutes after dropping 100 μ l chloroform on PDMS entrapped polystyrene-co-poly (dimethylacrylamide) core-shell nanoparticles

Experimental results show that core-shell nanoparticles are capable of being deposited onto a glass substrate. Additionally, substituting the curing agent (Part B) of a poly (dimethylsiloxane) PDMS elastomer kit from Dow Corning (Sylgard 184) for silicone (GE silicone SF96; viscosity, 50 cSt) reduces the need for unnecessary reagents. This change is significant because it shows that the curing agent (part B) has a similar viscosity and specific gravity as the silicone (50cSt viscosity; 0.97 g/ml specific gravity) used in the previous crystallization method.

4.0 Conclusions and Future Considerations

This thesis provides the foundation for the ultimate development of colorimetric biosensors capable of detecting pathogens. Because the goal of this work is to make abiotic sensors that undergo a structural change resulting in a color change that can be observed by the unaided human eye, the sensors will become useful in the detection of pathogens in low-resource settings. The principles established in this work, including the ability to synthesize hydrophobic core-hydrophilic shell monodisperse nanoparticles that crystallize and form a monochromatic (green) synthetic opal entrapped in PDMS which can change to a red color in less than 30 seconds upon the swelling of the PDMS elastomer matrix, promise that further investigations will likely lead to the development of successful colorimetric biosensors.

By covering the background regarding the physics that control structural color, the Hard Sphere and Soft Sphere models and their assembly into lattice structure, and the integration of synthetic opals into an elastomer matrix, this thesis paves the way for future considerations including the continued investigation into deposition methods that can take advantage of the core-shell interactions such as ink jet printing in order to develop multiple or multiplexed “litmus test” assays. Additionally, future work can include strategically cross-linking a gel matrix with hybridized dioligonucleotides that are displaced by competitive probe oligonucleotides as a method of controlling the expansion and shrinkage of the gel matrix. As such, colorimetric nanoparticles have a fascinating role to play in

bioengineering future biosensors for use as point-of-sample, low-cost, and easy-to-use diagnostics for pathogen detection.

Bibliography

1. Fudouzi H. Tunable structural color in organisms and photonic materials for design of bioinspired materials. *Science and Technology of Advanced Materials*. 2011;12(6):064704.
2. Byrne ME, Park K, Peppas NA. Molecular imprinting within hydrogels. *Advanced drug delivery reviews*. 2002;54(1):149-61.
3. Jillavenkatesa A, Dapkunas SJ, Lin-sien HL. NIST recommended practice guide special publication 960-1 Particle size characterization 2001.
4. Shen W, Li M, Ye C, Jiang L, Song Y. Direct-writing colloidal photonic crystal microfluidic chips by inkjet printing for label-free protein detection. *Lab on a Chip*. 2012;12(17):3089-95.
5. Holtz JH, Asher SA. Polymerized colloidal crystal hydrogel films as intelligent chemical sensing materials. *Nature*. 1997;389(6653):829-32.
6. Pedrotti FL. *Introduction To Optics*, 3/E: Pearson Education India; 2008.
7. Matsubara T, Oishi T, Katagiri A. Determination of porosity of TiO₂ films from reflection spectra. *Journal of The Electrochemical Society*. 2002;149(2):C89-C93.
8. Aguirre CI, Reguera E, Stein A. Tunable colors in opals and inverse opal photonic crystals. *Advanced Functional Materials*. 2010;20(16):2565-78.
9. Wang H, Zhang KQ. Photonic crystal structures with tunable structure color as colorimetric sensors. *Sensors*. 2013;13(4):4192-213. doi: 10.3390/s130404192. PubMed PMID: 23539027; PubMed Central PMCID: PMC3673079.
10. Bazin G, Zhu XX. Crystalline colloidal arrays from the self-assembly of polymer microspheres. *Progress in Polymer Science*. 2013;38(2):406-19. doi: 10.1016/j.progpolymsci.2012.09.002.
11. Weissman JM, Sunkara HB, Albert ST, Asher SA. Thermally switchable periodicities and diffraction from mesoscopically ordered materials. *Science*. 1996;274(5289):959-63.
12. Xia Y, Gates B, Yin Y, Lu Y. Monodispersed colloidal spheres: old materials with new applications. *Advanced Materials*. 2000;12(10):693-713.
13. Reese CE, Guerrero CD, Weissman JM, Lee K, Asher SA. Synthesis of highly charged, monodisperse polystyrene colloidal particles for the fabrication of photonic crystals. *Journal of colloid and interface science*. 2000;232(1):76-80.
14. Velev OD, Lenhoff AM, Kaler EW. A class of microstructured particles through colloidal crystallization. *Science*. 2000;287(5461):2240-3.
15. Ma C, Jiang Y, Yang X, Wang C, Li H, Dong F, et al. Centrifugation-induced water-tunable photonic colloidal crystals with narrow diffraction bandwidth and highly sensitive detection of SCN⁻. *ACS applied materials & interfaces*. 2013;5(6):1990-6. doi: 10.1021/am302804b. PubMed PMID: 23448168.
16. Wang T, Keddie JL. Design and fabrication of colloidal polymer nanocomposites. *Advances in colloid and interface science*. 2009;147:319-32.
17. Fudouzi H. Fabricating high-quality opal films with uniform structure over a large area. *Journal of colloid and interface science*. 2004;275(1):277-83.
18. Fudouzi H, Xia Y. Colloidal crystals with tunable colors and their use as photonic papers. *Langmuir*. 2003;19(23):9653-60.

19. Tierney S, Stokke BT. Development of an oligonucleotide functionalized hydrogel integrated on a high resolution interferometric readout platform as a label-free macromolecule sensing device. *Biomacromolecules*. 2009;10(6):1619-26.
20. Njenga HN, Wanasolo W. MODULE 13 INDUSTRIAL CHEMISTRY.
21. Peiffer D, Kim M, Kaladas J. Synthesis, solution viscosity and interfacial properties of random copolymers spanning a broad range of anionic character. *Polymer*. 1988;29(4):716-23.